engineering proceedings

MDPI

Proceeding Paper

Artificial Intelligence-Enhanced Contactless Screening Kiosks: Leveraging Machine Learning for Infectious Disease Detection and Mitigation †

Marisol Jane M. Beray [1,*], Ramil B. Arante [1] and Jofel Batutay [2]

[1] Department of Teacher Education, Caraga State University, Cabadbaran City 8605, Philippines; rbarante@carsu.edu.ph
[2] Department of Computer Applications, Iligan Institute of Technology, Mindanao State University, Iligan City 9700, Philippines; jofel.batutay@g.msuiit.edu.ph
* Correspondence: marisoljane.beray@carsu.edu.ph
† Presented at the 8th International Global Conference Series on ICT Integration in Technical Education & Smart Society, Aizuwakamatsu City, Japan, 20–26 January 2026.

Abstract

The COVID-19 pandemic exposed critical limitations in conventional screening protocols, particularly in high-traffic environments where rapid, accurate, and contactless health assessment became essential to mitigate transmission risks. In response, this study presents the development of an Artificial Intelligence-Enhanced Contactless Screening Kiosk (AICS-K) that integrates multimodal sensing, embedded systems engineering, and machine learning into a unified workflow. Utilizing a Raspberry Pi platform with computer vision, thermal sensing, QR-based contact tracing, and intelligent control logic, the system enables efficient real-time screening while minimizing human intervention. The proposed architecture demonstrates the potential of extensible, affordable AI-driven solutions for early signs detection and institutional health resilience.

Keywords: artificial intelligence; embedded systems; contactless screening; machine learning; thermal imaging; QR-based contact tracing; infectious disease mitigation

1. Introduction

The COVID-19 pandemic exposed critical limitations in conventional screening protocols [1], particularly in high-traffic environments where rapid, accurate, and contactless assessment was essential [2–6]. Manual workflows, such as hand-held thermometers, paper-based contact-tracing forms, and hand-spraying, not only slowed throughput but also increased exposure risk to staff. To overcome these challenges, researchers began to explore embedded system architectures that could integrate multiple sensing modalities into a unified, automated workflow [3,6,7].

At the core of such systems is the embedded controller, typically a Raspberry Pi or similar single-board computer, which orchestrates sensor inputs, machine learning inference, and actuator outputs [8]. Thermal imaging modules provide non-contact temperature measurement, while RGB cameras enable face localization and mask detection. Ultrasonic sensors enforce social distancing compliance, and QR code scanners facilitate digital contact tracing. These components are connected through GPIO interfaces and I^2C/SPI buses, forming a tightly coupled embedded system capable of real-time operation. Studies confirm that multimodal fusion, which maps RGB face detections to thermal regions of

Check for updates

Academic Editors: Debopriyo Roy, George Fragulis and Peter Ilic

Published: 10 June 2026

Copyright: © 2026 by the authors. Licensee MDPI, Basel, Switzerland. This article is an open access article distributed under the terms and conditions of the Creative Commons Attribution (CC BY) license.

interest, significantly improves measurement reliability compared to single-point thermal reads [9–12].

The embedded software stack is equally critical. Lightweight computer vision algorithms, implemented in OpenCV (v4.0), perform face detection and QR decoding, while quantized deep learning models such as MobileNetV2 (v1.0) run on TensorFlow Lite to detect mask usage efficiently on constrained hardware [13]. Control logic is implemented as a finite state machine, guiding the workflow from user approach to temperature capture, QR logging, sanitizer actuation, and exit. This architecture ensures deterministic behavior, low latency, and modularity for upgrades. Drive-through and kiosk-based triage studies have demonstrated that such automation can reduce staff exposure and improve throughput, validating the embedded system approach [2,3].

Beyond sensing and actuation, the architecture incorporates a web-backed database for QR token storage and audit logging. Privacy-preserving design principles are applied, storing only minimal identifiers (QR token, timestamp, temperature) to balance contact tracing utility with institutional data protection requirements [14–17]. Reviews of digital contact tracing interventions emphasize that adoption and effectiveness increase when systems minimize personal data retention and integrate seamlessly into institutional workflows [16].

Taken together, the embedded system design of the AICS-K demonstrates how commodity hardware, multimodal sensing, and lightweight machine learning can be fused into a low-cost, modular architecture. This approach directly addresses the limitations of manual workflows and the prohibitive cost of commercial kiosks, offering an extensible solution for universities, small businesses, and community facilities.

2. Related Works

2.1. Limitations of Manual Screening and the Rise in Automation

Manual screening methods—such as handheld thermometers, paper contact-tracing forms, and hand-spraying—are widely acknowledged to be inefficient and risky. Aggarwal et al. conducted a systematic review of non-contact infrared thermometers and thermal scanners, revealing significant variability in diagnostic accuracy due to environmental factors and inconsistent measurement protocols [1]. These limitations underscore the need for automated systems that can standardize screening procedures and reduce human error.

Kwon et al. demonstrated the effectiveness of drive-through screening centers in South Korea, where automation significantly reduced staff exposure and improved throughput during mass outbreaks [2]. Their findings support the broader adoption of kiosk-based triage systems, particularly in high-traffic environments such as universities and government offices [3,5,18].

2.2. Thermal Imaging and Sensor Fusion

Thermal imaging has become a cornerstone of contactless screening systems. However, its effectiveness depends heavily on sensor placement, resolution, and calibration [19]. Clinical and methodological studies emphasized the importance of facial region selection in thermal screening, noting that measurement accuracy improves when the thermal region of interest (ROI) is precisely mapped to the forehead [6]. This insight informs the AICS K's use of RGB-to-thermal fusion, where face detection guides ROI selection on a low-resolution thermal array (e.g., AMG8833), enhancing reliability despite hardware constraints.

To compensate for the limitations of low-cost sensors, researchers have proposed signal processing techniques such as bicubic interpolation, temporal smoothing, and per-session offset calibration [11,12,19–24]. These methods have been shown to reduce systematic

bias and improve repeatability, making them suitable for embedded systems deployed in institutional settings.

2.3. Digital Contact Tracing and QR-Based Systems

Digital contact tracing emerged as a critical tool during the pandemic, with QR-based and mobile-app-based systems gaining widespread attention because of their scalability and privacy implications [25]. Reviews in this area have consistently emphasized the tension between epidemiological usefulness, privacy, and user adoption [15,26]. The AICS-K aligns with these findings by storing only minimal identifiers needed for institutional logging.

Related embedded access-control solutions have shown that contactless logging, disinfection, and mask detection can be integrated into a unified workflow. These studies support the practical value of combining sensing, logging, and automated actuation into one system rather than relying on fragmented manual steps.

2.4. Lightweight Machine Learning for Edge Deployment

The integration of machine learning into embedded systems has enabled real-time inference on constrained hardware. Studies using MobileNetV2, transfer learning, and other lightweight architectures have shown that mask detection can be performed efficiently on edge devices such as Raspberry Pi platforms [27–30]. This supports the AICS-K's use of quantized MobileNetV2 models running on TensorFlow Lite for on-device mask detection.

Other studies have explored the use of deep learning for face recognition, masked-face analysis, thermal anomaly detection, and embedded vision pipelines. Across this literature, lightweight and deployable models are generally favored for edge deployment, especially in resource-constrained environments where latency, power consumption, cost, and privacy remain critical design concerns [31].

3. Methods

This section describes the procedures undertaken in the development of which focuses on designing a modular embedded system that integrates multiple sensing modalities, lightweight machine learning, and automated actuation into a unified workflow. Its architecture emphasizes affordability, scalability, and maintainability, making it suitable for deployment in universities, small businesses, and community facilities.

3.1. System Architecture

3.1.1. Embedded Controller and Core Processing

At the heart of the kiosk is a Raspberry Pi 4 Model B, which serves as the central embedded controller. This single-board computer orchestrates sensor inputs, executes machine-learning inference, and manages actuator outputs. The Pi's GPIO pins and I^2C/SPI buses provide direct interfaces to peripheral sensors, while USB and HDMI ports support camera modules and display units. The choice of Raspberry Pi ensures low cost, wide availability, and compatibility with open-source software libraries.

3.1.2. Sensor Subsystems

The kiosk integrates several sensor modules to achieve multimodal screening:

- Thermal Imaging: An AMG8833 infrared thermal array captures non-contact temperature readings. Although limited to an 8×8 grid, interpolation and calibration routines enhance accuracy.
- RGB Camera: A Raspberry Pi Camera Module V2 provides visual input for face localization and QR code scanning.

https://doi.org/10.3390/engproc2026143005

- Ultrasonic Sensor: An HC SR04 module enforces queue spacing and triggers sanitizer actuation when a user approaches.
- QR Scanner: Implemented via the RGB camera and OpenCV's zbar library, enabling digital contact tracing through QR tokens.
- These sensors are tightly coupled through the embedded controller, forming a multimodal sensing pipeline that reduces false positives and improves reliability compared to a single modality.

3.1.3. Actuation and Feedback

The kiosk includes an automatic alcohol dispenser triggered by ultrasonic sensing, ensuring touch-free sanitization. A 7-inch HDMI LCD display provides real-time feedback, while audio prompts guide users through the screening process. This combination of visual and auditory feedback improves usability and compliance.

3.1.4. Software Stack and Machine Learning Integration

The embedded software stack is built on Raspberry Pi OS Buster 64-bit with Python v3.8.2 and C++ libraries v11.

- Computer Vision: OpenCV performs face detection, QR decoding, and ROI mapping between RGB and thermal frames.
- Machine Learning: A quantized MobileNetV2 model runs on TensorFlow Lite, enabling real time mask detection on constrained hardware [31–34].
- Control Logic: A finite state machine governs the workflow: idle → approach detection → face localization → thermal capture → QR scan → sanitizer actuation → logging. This deterministic logic ensures low latency and predictable operation.

Figure 1 Shows the flowchart of the AI-based models and experimental methods applied.

This system's integration of face detection via Haar cascades with subsequent temperature measurement using a thermal camera, and QR code scanning for data validation and transmission reflects a common design pattern in automated access control and health monitoring applications developed during and after the COVID-19 period [14,34]. Related work has used OpenCV-based face detection, embedded machine learning, and QR-assisted logging in screening and access workflows, supporting the technical feasibility of combining these functions within a single low-cost embedded system.

Advancements in infrared thermal imaging have further supported these architectures by enabling more consistent fever screening and physiological monitoring in public or clinical settings [6]. Research on thermal measurement, facial region selection, and screening standardization shows that careful sensor placement and calibration are essential to reliable deployment, especially under changing environmental conditions. These methodologies underscore the importance of robust initialization, error handling, and multimodal integration in real-world deployments. Related embedded and computer-vision studies further suggest that face detection, mask recognition, and database-backed logging are increasingly converging in practical edge-AI systems [29,32–34].

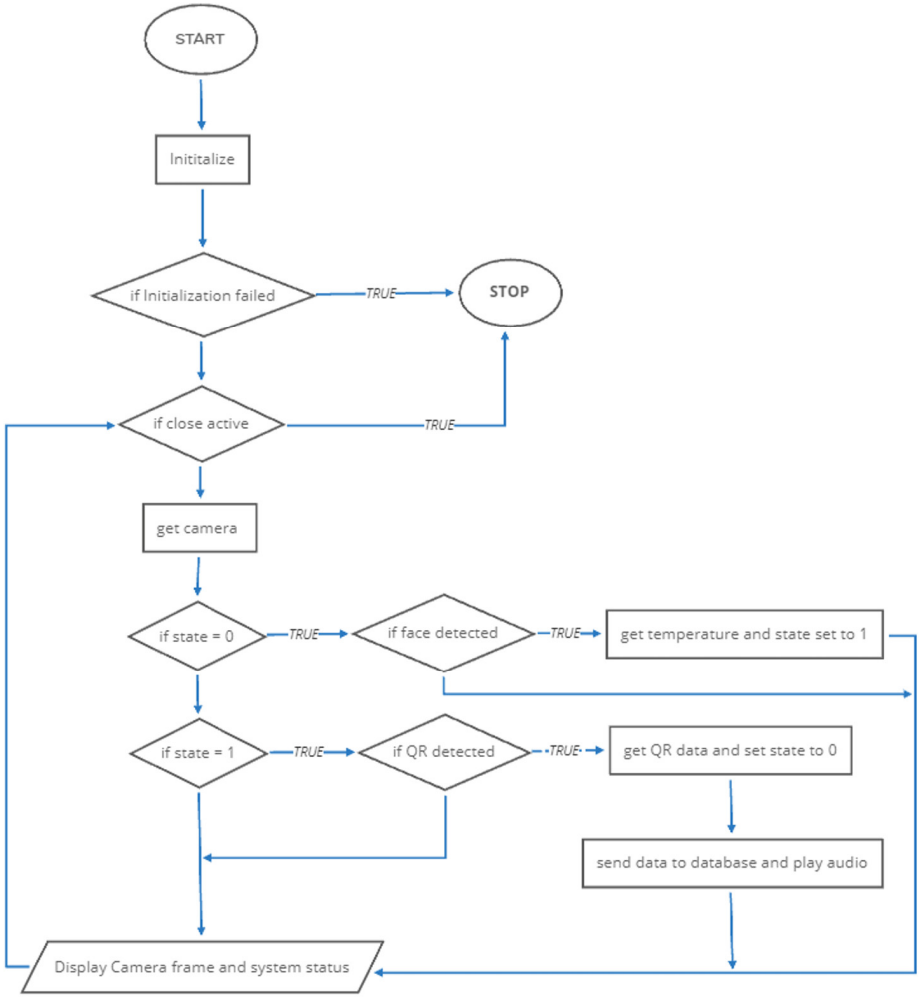


Figure 1. The flowchart of the AI-based models and experimental methods applied.

3.1.5. Web Development

The system underwent rigorous testing using XAMPP v7.4.3 throughout its development phase, ensuring robust functionality before transitioning to an online server to enable accessibility for users with internet connectivity. This deployment strategy aligns with modern web-based health monitoring frameworks, facilitating real-time data collection and remote access. The database architecture is structured around two primary tables: a user table and a data table. The user table comprehensively stores individual attributes such as identification, name, contact details, and demographic information, serving as the foundation for personalized QR code generation. The data table captures dynamic inputs, including timestamps, temperature readings, and data type classifications, which are recorded when a user interacts with the developed device. This relational design, depicted in the Entity Relationship Diagram (ERD) in Figure 2, establishes a one-to-many relationship between users and their associated data entries, optimizing data integrity and retrieval efficiency. Such a schema supports extensible health screening applications, as evidenced by similar systems employing relational databases for tracking patient vitals and QR-based authentication in public health settings. The integration of XAMPP v7.4.3 with MySQL (MariaDB v10.4.11) ensures a secure, portable environment for local testing, while the online migration leverages cloud-based scalability, addressing latency and concurrency challenges in high-traffic scenarios.

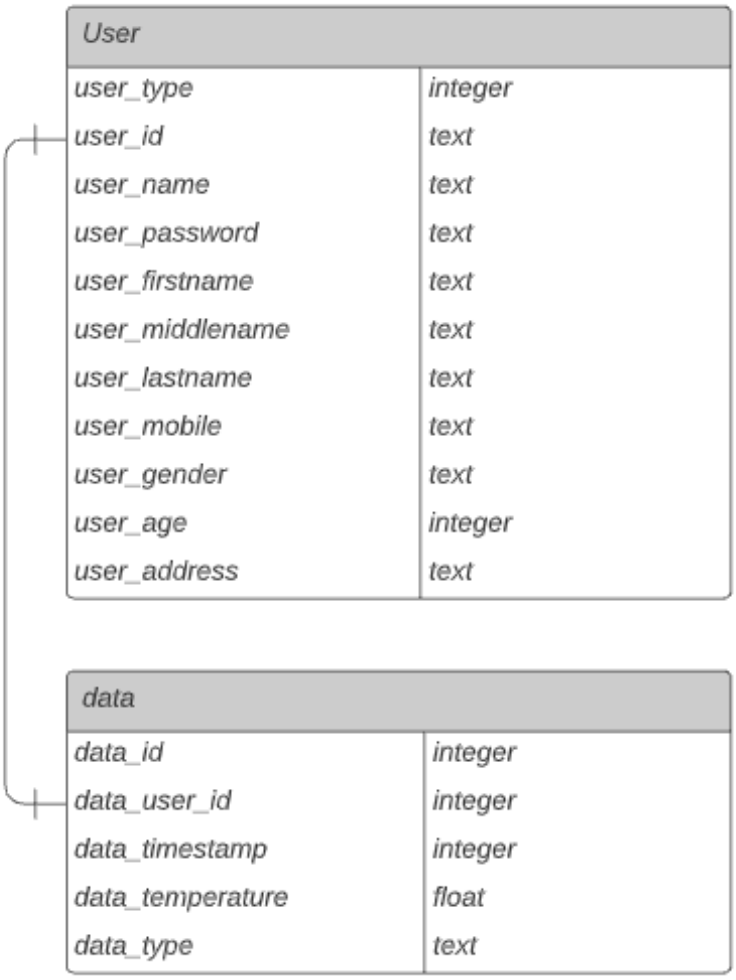


Figure 2. Entity Relationship Diagram.

3.1.6. Data Management and Privacy

A lightweight PHP/MySQL backend stores QR tokens, timestamps, and temperature readings. Privacy-preserving design principles are applied, retaining only minimal identifiers to balance contact-tracing utility with institutional data-protection requirements. Reviews of digital contact-tracing interventions emphasize that such privacy safeguards are essential for adoption.

3.1.7. Operational Workflow

The kiosk's workflow begins when the ultrasonic sensor detects a user's approach. The RGB camera localizes the face, mapping the ROI to the thermal array for accurate temperature estimation. If the reading exceeds a threshold, the system issues a warning. The user then presents a QR code, which is decoded and logged. Finally, the sanitizer dispenser is triggered, and the system records the transaction before resetting to idle. This workflow reduces per-person screening time to approximately 14 s, compared to 25–30 s for manual workflows.

At the center of the design is the embedded controller, a Raspberry Pi 4 Model B. This single-board computer acts as the hub of the system, coordinating all sensor inputs, executing machine learning inference, and managing actuator outputs. Its GPIO, I^2C, and SPI interfaces allow direct communication with peripheral sensors, while HDMI and USB ports support the display and camera modules. The Raspberry Pi was chosen for its balance of computational capability, affordability, and compatibility with open-source libraries, making it ideal for institutional deployments. On the other hand, surrounding

the controller are the sensor subsystems that provide multimodal input [8]. The AMG8833 infrared thermal array captures non-contact temperature readings, which are enhanced through interpolation and calibration routines to improve accuracy despite the sensor's low resolution [21,35]. The Pi Camera V2 supplies RGB images used for face localization, QR code scanning, and mask detection. An HC SR04 ultrasonic sensor detects user approach and enforces queue spacing, while QR decoding is performed through the RGB camera using OpenCV's zbar library [36]. Together, these sensors form a multimodal pipeline that reduces false positives and improves reliability compared to single modality systems.

On the output side, the kiosk integrates actuation and feedback mechanisms. An automatic sanitizer dispenser, triggered by ultrasonic sensing, ensures touch-free hand disinfection [37]. A 7-inch HDMI LCD provides visual instructions, while audio prompts guide users through each step of the process. This multimodal feedback enhances usability and compliance, ensuring that users follow the screening protocol correctly.

The software stack running on the Raspberry Pi OS ties these components together. OpenCV libraries handle computer vision tasks such as face detection, QR decoding, and ROI mapping between RGB and thermal frames. A quantized MobileNetV2 model, deployed via TensorFlow Lite, enables real-time mask detection on constrained hardware [13,38]. Control logic is implemented as a finite state machine, governing the workflow from idle state to approach detection, face localization, thermal capture, QR scan, sanitizer actuation, and logging. Moreover, for data management and privacy, a lightweight PHP/MySQL backend stores QR tokens, timestamps, and temperature readings. Privacy-preserving principles are applied, retaining only minimal identifiers to balance contact tracing utility with institutional data protection requirements. Reviews of digital contact tracing interventions emphasize that such safeguards are essential for adoption [27].

Finally, the operational workflow depicted in Figure 3 begins when the ultrasonic sensor detects a user's approach. The RGB camera localizes the face, mapping the ROI to the thermal array for accurate temperature estimation. If the reading exceeds a threshold, the system issues a warning. The user then presents a QR code, which is decoded and logged in the backend database. The sanitizer dispenser is triggered automatically, and the transaction is recorded before the system resets to idle. Prototype evaluations report average screening times of approximately 14 s per person compared to 25–30 s for manual workflows.

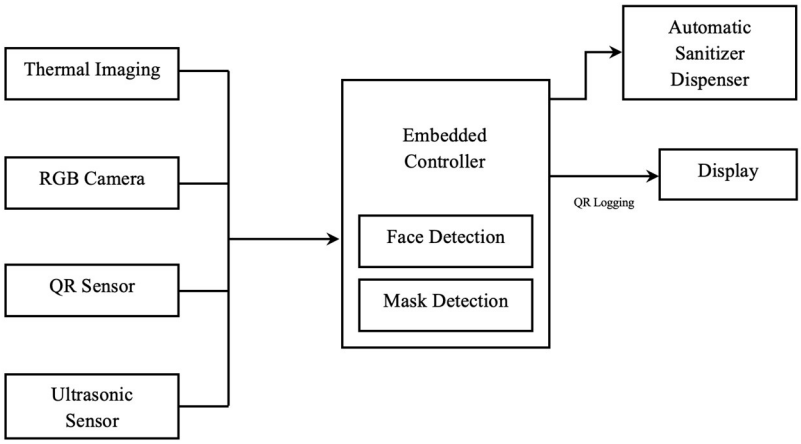


Figure 3. This is the Block Diagram of the System Architecture showing how the embedded controller, sensor subsystems, machine learning pipeline, actuators, and backend database interact to deliver a seamless screening workflow.

4. Results

4.1. Screening Throughput and End-to-End Transaction Time

The first key outcome of the Artificial Intelligence-Enhanced Contactless Screening Kiosk (AICS-K) is its improvement in end-to-end screening efficiency. Based on the prototype evaluation underlying this study, the kiosk completed one full screening cycle in an average of 14.09 s, whereas the conventional manual procedure required approximately 25–30 s per person. This result indicates that the integration of ultrasonic triggering, face localization, temperature capture, QR logging, and sanitizer actuation into a single embedded workflow improves throughput relative to fragmented manual screening. Such improvement is consistent with previous reports that automated and kiosk-based screening systems can reduce staff exposure and improve operational efficiency during public health emergencies.

The total transaction time of the kiosk can be expressed in Equation (1):

$$T_{\mathrm{AICS-K}} \approx T_u + T_f + T_m + T_q + T_d + T_b + T_{\mathrm{dbg}}, \quad (1)$$

where T_u denotes ultrasonic detection time, T_f denotes face localization time, T_m denotes temperature and mask-check time, T_q denotes QR decoding time, T_d denotes sanitizer dispensing time, T_b denotes backend logging time, and T_{dbg} denotes debug overhead [39,40]. Using the observed average transaction time, the approximate throughput of the system is:

$$\text{Throughput} = \tfrac{60}{14.09} \approx 4.26 \text{ persons/min}. \quad (2)$$

This throughput is appropriate for institutional entrances where stable, contactless, and repeatable screening is more important than high-density crowd scanning. The result also supports the practical suitability of the AICS-K for universities, offices, and similar environments where moderate but continuous traffic must be handled efficiently.

4.2. Computational Efficiency of the Embedded Processing Pipeline

The second result concerns the computational behavior of the embedded screening pipeline. The Tentative performance analysis indicates that each major subsystem, like ultrasonic detection, face localization, temperature and mask assessment, QR code scanning, database transaction, and debug delay, which operates with constant-time complexity O(1) because each stage processes either fixed-size sensor input or a single fixed-resolution image frame. The same analysis further notes that the core embedded logic and machine learning inference are complete in under 5 s, implying that most of the total user interaction time is attributable to practical operating conditions rather than to computational scaling [38,39].

The computational behavior may therefore be summarized as shown in Equations (3) and (4) [41].

$$T_{\mathrm{core}} = O(1), \quad (3)$$

or, more explicitly,

$$T_{\mathrm{core}} = T_u + T_f + T_m + T_q + T_b. \quad (4)$$

Because each of these components is bounded by a fixed computational cost, the per-user processing load does not increase with continued system operation. This is a desirable property for edge deployment because it ensures predictable latency and stable performance over time [38]. The result is also aligned with the system architecture described in the paper, where the Raspberry Pi controller, OpenCV computer vision pipeline, TensorFlow Lite inference engine, and finite-state machine are deliberately selected to support lightweight and deterministic operation. From a systems engineering perspective, this confirms that the

AICS-K is not only functionally integrated but also computationally suitable for low-cost embedded deployment.

4.3. Environmental and User-Dependent Effects on QR Decoding Performance

Although the embedded logic exhibits constant-time behavior, the observed end-to-end transaction time is influenced by several environmental and user-dependent factors, especially during QR code acquisition. The Tentative analysis identifies ambient lighting, camera-to-code distance and angle, user device screen brightness, and debug overhead as the primary contributors to delay in the QR decoding stage [39]. As shown in Equation (5), the effective QR processing time can therefore be modeled as

$$T'_q = T_q + \Delta L + \Delta\theta + \Delta B + \Delta_{\text{dbg}}, \tag{5}$$

where ΔL denotes lighting-related delay, Δθ represents delay due to distance and angular misalignment, ΔB denotes delay caused by insufficient screen brightness from the user's device, and Δ_{dbg} represents fixed debug overhead. Among these variables, user device brightness was identified as the largest practical source of delay, because low screen brightness reduces QR contrast and forces the user to reposition the device or manually adjust the display before successful acquisition.

This finding explains the gap between the sub-5 s internal processing time and the observed average end-to-end transaction time of 14.09 s. It also shows that system performance in real deployments depends not only on algorithmic efficiency but also on the human–device interaction at the acquisition stage [40]. Accordingly, future design improvements may include better front illumination, adaptive camera exposure control, or interface prompts instructing users to maximize screen brightness before scanning. Such refinements would likely reduce QR-related delay and bring the total transaction time closer to the intrinsic processing speed of the embedded system.

4.4. Multimodal Reliability and Functional Integration

The fourth result concerns the reliability of the multimodal screening workflow. The AICS-K integrates ultrasonic sensing, computer vision, thermal imaging, QR-based identity logging, and automated sanitizer actuation into a single sequential process. Prototype evaluation from the source study reported a temperature difference of only 0.1–0.2 °C relative to a commercial temperature device, as well as successful QR detection and decoding in all 11 observed trials. The same source also reported highly acceptable ratings for design, functionality, and usability, indicating stable functional performance during expert assessment.

A simplified reliability representation for the serial workflow can be written as Equation (6):

$$R_{\text{sys}} = R_u \cdot R_f \cdot R_m \cdot R_q \cdot R_b, \tag{6}$$

where R_u, R_f, R_m, R_q, and R_b denote the reliabilities of ultrasonic detection, face localization, temperature and mask assessment, QR decoding, and backend logging, respectively [41]. Because the workflow is sequential, degradation in any one stage directly affects the success of the complete screening transaction [42]. Nevertheless, the reported temperature agreement, complete QR decoding success in the observed trials, and strong acceptability results suggest that the multimodal architecture performs reliably enough for controlled institutional use.

Taken together, these findings indicate that the AICS-K benefits from the combined strengths of multiple low-cost sensing modalities as presented in Table 1. Face localization improves the relevance of thermal measurement, QR logging strengthens traceability, and

embedded automation reduces dependence on manual operators. The results therefore support the view that the system's operational effectiveness arises not from any single sensor alone but from the coordinated integration of sensing, inference, actuation, and logging within one embedded platform.

Table 1. Summary of key AICS-K performance results.

Metric	Result	Basis
Average full screening time	14.09 s	Prototype evaluation
Manual screening time	25–30 s	Comparative baseline
Estimated throughput	4.26 persons/min	Computed from Equation (2)
Core processing time	<5 s	Runtime analysis
Temperature difference vs. commercial device	0.1–0.2 °C	Calibration result
QR decoding success	11/11 trials	QR validation
Dominant runtime variability factor	User device brightness	Tentative analysis

5. Conclusions

The study demonstrates that the developed system reduced the average screening time compared to doing manual procedures, while also showing a reported temperature difference relative to a commercial device and successful QR decoding in all observed trials. These findings support the functional feasibility of the developed kiosk for contactless institutional screening. However, the results were obtained from prototype testing and limited observations; thus, broader validation is recommended. Future work shall focus on larger-scale field testing, improved QR acquisition under varying light conditions, and further refinement of the overall system design.

Author Contributions: Conceptualization, M.J.M.B., J.B. and R.B.A.; related works, R.B.A.; software, J.B.; validation, M.J.M.B. and J.B.; formal analysis, M.J.M.B., J.B. and R.B.A.; investigation, M.J.M.B. and J.B.; resources, R.B.A.; data curation, M.J.M.B.; writing—original draft preparation, M.J.M.B., J.B. and R.B.A.; writing—review and editing, R.B.A.; visualization, J.B.; supervision, M.J.M.B. and R.B.A. All authors have read and agreed to the published version of the manuscript.

Funding: This research was funded by Caraga State University, Cabadbaran Campus, with a grant amounting to ₱54,115.00.

Institutional Review Board Statement: Not applicable.

Informed Consent Statement: Informed consent was obtained from all subjects involved in the study.

Data Availability Statement: The datasets used and analyzed during the current study are available from the corresponding author upon reasonable request.

Acknowledgments: The authors gratefully acknowledge Caraga State University Cabadbaran Campus for its institutional support of this research. The authors also extend their appreciation to the technical staff, administrative personnel, and expert evaluators whose assistance and professional insights contributed to the development, testing, and evaluation of the Artificial Intelligence-Enhanced Contactless Screening Kiosk (AICS-K). During the preparation of this manuscript, the authors used ChatGPT (GPT-5.4 Thinking, OpenAI) for language refinement and manuscript organization. The authors have reviewed and edited the output and take full responsibility for the content of this publication.

Conflicts of Interest: The authors declare no conflicts of interest.

Abbreviations

The following abbreviations are used in this manuscript:

AICS-K	Artificial Intelligence-Enhanced Contactless Screening Kiosk
AI	Artificial Intelligence
AMG8833	Panasonic infrared thermal array sensor
CNN	Convolutional Neural Network
ERD	Entity Relationship Diagram
GPIO	General Purpose Input/Output
HDMI	High-Definition Multimedia Interface
I^2C	Inter-Integrated Circuit
LCD	Liquid Crystal Display
PHP	Hypertext Processor
QR	Quick Response
RGB	Red, Green, Blue
ROI	Region of Interest
SPI	Serial Peripheral Interface
XAMPP	Cross-Platform, Apache, MariaDB/MySQL, PHP, and Perl

References

1. Alvarez, E.; Bielska, I.A.; Hopkins, S.; Belal, A.A.; Goldstein, D.M.; Slick, J.; Pavalagantharajah, S.; Wynfield, A.; Dakey, S.; Gedeon, M.-C.; et al. Limitations of COVID-19 testing and case data for evidence-informed health policy and practice. *Health Res. Policy Syst.* **2023**, *21*, 11. [CrossRef]
2. Kwon, K.T.; Ko, J.-H.; Shin, H.; Sung, M.; Kim, J.Y. Drive-Through Screening Center for COVID-19: A Safe and Efficient Screening System against Massive Community Outbreak. *J. Korean Med. Sci.* **2020**, *35*, e123. [CrossRef]
3. Budd, J.; Miller, B.S.; Manning, E.M.; Lampos, V.; Zhuang, M.; Edelstein, M.; Rees, G.; Emery, V.C.; Stevens, M.M.; Keegan, N.; et al. Digital technologies in the public-health response to COVID-19. *Nat. Med.* **2020**, *8*, 1183–1192. [CrossRef]
4. A Lewnard, J.; Lo, N.C. Scientific and ethical basis for social-distancing interventions against COVID-19. *Lancet Infect. Dis.* **2020**, *20*, 631. [CrossRef]
5. Manigandan, S.; Wu, M.-T.; Ponnusamy, V.K.; Raghavendra, V.B.; Pugazhendhi, A.; Brindhadevi, K. A systematic review on recent trends in transmission, diagnosis, prevention and imaging features of COVID-19. *Process Biochem.* **2020**, *98*, 233–240. [CrossRef]
6. Aggarwal, N.; Garg, M.; Dwarakanathan, V.; Gautam, N.; Kumar, S.S.; Jadon, R.S.; Gupta, M.; Ray, A. Diagnostic accuracy of non-contact infrared thermometers and thermal scanners: A systematic review and meta-analysis. *J. Travel Med.* **2020**, *27*, taaa193. [CrossRef]
7. Khaksari, K.; Nguyen, T.; Hill, B.Y.; Perrault, J.; Gorti, V.; Blick, E.; Cano, T.G.; Shadgan, B.; Quang, T.; Malpani, R.; et al. Review of the efficacy of infrared thermography for screening infectious diseases with applications to COVID-19. *J. Med. Imaging* **2021**, *8*, 010901. [CrossRef] [PubMed]
8. Mathe, S.E.; Kondaveeti, H.K.; Vappangi, S.; Vanambathina, S.D.; Kumaravelu, N.K. A comprehensive review on applications of Raspberry Pi. *Comput. Sci. Rev.* **2024**, *52*, 100636. [CrossRef]
9. Dzien, C.; Halder, W.; Winner, H.; Lechleitner, M. COVID-19 screening: Are forehead temperature measurements during cold outdoor temperatures really helpful? *Wien. Klin. Wochenschr.* **2020**, *133*, 331. [CrossRef] [PubMed]
10. Priest, P.C.; Duncan, A.R.; Jennings, L.C.; Baker, M.G. Thermal Image Scanning for Influenza Border Screening: Results of an Airport Screening Study. *PLoS ONE* **2011**, *6*, e14490. [CrossRef] [PubMed]
11. Zhou, Y.; Ghassemi, P.; Chen, M.; McBride, D.; Casamento, J.P.; Pfefer, T.J.; Wang, Q. Clinical evaluation of fever-screening thermography: Impact of consensus guidelines and facial measurement location. *J. Biomed. Opt.* **2020**, *25*, 097002. [CrossRef]
12. Foster, J.; Lloyd, A.B.; Havenith, G. Non-contact infrared assessment of human body temperature: The journal Temperature toolbox. *Temp. Multidiscip. Biomed. J.* **2021**, *8*, 306. [CrossRef]
13. Sandler, M.; Howard, A.; Zhu, M.; Zhmoginov, A.; Chen, L. MobileNetV2: Inverted Residuals and Linear Bottlenecks. In *Proceedings of the IEEE Computer Society Conference on Computer Vision and Pattern Recognition*; IEEE: Salt Lake City, UT, USA, 2018; pp. 4510–4520. [CrossRef]
14. Nakamoto, I.; Wang, S.; Guo, Y.; Zhuang, W. A QR Code-Based Contact Tracing Framework for Sustainable Containment of COVID-19: Evaluation of an Approach to Assist the Return to Normal Activity. *JMIR Mhealth Uhealth* **2020**, *8*, e22321. [CrossRef]
15. Bardus, M.; Al Daccache, M.; Maalouf, N.; Al Sarih, R.; Elhajj, I.H. Data Management and Privacy Policy of COVID-19 Contact-Tracing Apps: Systematic Review and Content Analysis. *JMIR Mhealth Uhealth* **2022**, *10*, e35195. [CrossRef]

16. Akinbi, A.; Forshaw, M.; Blinkhorn, V. Contact tracing apps for the COVID-19 pandemic: A systematic literature review of challenges and future directions for neo-liberal societies. *Health Inf. Sci. Syst.* **2021**, *9*, 18. [CrossRef]
17. Tsvyatkova, D.; Buckley, J.; Beecham, S.; Chochlov, M.; O'kEeffe, I.R.; Razzaq, A.; Rekanar, K.; Richardson, I.; Welsh, T.; Storni, C.; et al. Digital Contact Tracing Apps for COVID-19: Development of a Citizen-Centered Evaluation Framework. *JMIR Mhealth Uhealth* **2022**, *10*, e30691. [CrossRef] [PubMed]
18. 2019 Novel Coronavirus Disease (COVID-19): Detection and Diagnosis System Using IoT Based Smart Glasses. Available online: https://www.researchgate.net/publication/340732271_2019_Novel_Coronavirus_Disease_Covid-19_Detection_and_Diagnosis_System_Using_IoT_Based_Smart_Glasses (accessed on 7 March 2026).
19. Ring, E.F.J.; Mcevoy, H.; Jung, A.; Zuber, J.; Machin, G. New standards for devices used for the measurement of human body temperature. *J. Med. Eng. Technol.* **2010**, *34*, 249–253. [CrossRef] [PubMed]
20. Zhao, Y.; Bergmann, J.H.M. Non-Contact Infrared Thermometers and Thermal Scanners for Human Body Temperature Monitoring: A Systematic Review. *Sensors* **2023**, *23*, 7439. [CrossRef] [PubMed]
21. Perpetuini, D.; Filippini, C.; Cardone, D.; Merla, A. An Overview of Thermal Infrared Imaging-Based Screenings during Pandemic Emergencies. *Int. J. Environ. Res. Public Health* **2021**, *18*, 3286. [CrossRef]
22. Chan, P.Y.; Tay, A.; Chen, D.; Vogrin, S.; McNeil, J.; Hopper, I. Comparison of cutaneous facial temperature using infrared thermography to standard temperature measurement in the critical care setting. *J. Clin. Monit. Comput.* **2021**, *36*, 1029. [CrossRef]
23. Antunes, A.C.M.; Aldred, A.; Moreno, G.P.T.; Ribeiro, J.A.d.S.; Brandão, P.E.; Barone, G.T.; Conselheiro, J.d.A.; Goulart, A.C.; Desuó, I.C.; Gomes, G. Potential of using facial thermal imaging in patient triage of flu-like syndrome during the COVID-19 pandemic crisis. *PLoS ONE* **2023**, *18*, e0279930. [CrossRef]
24. Aldred, A.; Ribeiro, J.A.S.; Bezerra, P.M.S.; Antunes, A.C.M.; Goulart, A.C.; Desuó, I.C.; Gomes, G. Application of thermography to estimate respiratory rate in the emergency room: The journal Temperature toolbox. *Temperature* **2022**, *10*, 159–165. [CrossRef]
25. Unim, B.; Zile-Velika, I.; Pavlovska, Z.; Lapao, L.; Peyroteo, M.; Misins, J.; Forjaz, M.J.; Nogueira, P.; Grisetti, T.; Palmieri, L. The role of digital tools and emerging devices in COVID-19 contact tracing during the first 18 months of the pandemic: A systematic review. *Eur. J. Public Health* **2024**, *34*, i11–i28. [CrossRef]
26. Nagrath, P.; Jain, R.; Madan, A.; Arora, R.; Kataria, P.; Hemanth, J. SSDMNV2: A real time DNN-based face mask detection system using single shot multibox detector and MobileNetV2. *Sustain. Cities Soc.* **2021**, *66*, 102692. [CrossRef]
27. Sethi, S.; Kathuria, M.; Kaushik, T. Face mask detection using deep learning: An approach to reduce risk of Coronavirus spread. *J. Biomed. Inform.* **2021**, *120*, 103848. [CrossRef]
28. Ullah, N.; Javed, A.; Ghazanfar, M.A.; Alsufyani, A.; Bourouis, S. A novel DeepMaskNet model for face mask detection and masked facial recognition. *J. King Saud Univ. Comput. Inf. Sci.* **2022**, *34*, 9905–9914. [CrossRef] [PubMed]
29. Schroff, F.; Kalenichenko, D.; Philbin, J. FaceNet: A unified embedding for face recognition and clustering. In Proceedings of the IEEE Computer Society Conference on Computer Vision and Pattern Recognition, Boston, MA, USA, 7–12 June 2015; pp. 815–823. [CrossRef]
30. Khalifa, A.F.; Badr, E.; Elmahdy, H.N. A survey on human detection surveillance systems for Raspberry Pi. *Image Vis. Comput.* **2019**, *85*, 1–13. [CrossRef]
31. Dubey, P.; Keswani, V.; Dubey, P.; Keswani, G.; Bhagat, D. Innovative IoT-enabled mask detection system: A hybrid deep learning approach for public health applications. *MethodsX* **2025**, *14*, 103291. [CrossRef] [PubMed]
32. Bolima, D.; Huerto, C.A. Contactless logging and disinfection solution with automated face mask detection. *Int. J. Electr. Comput. Eng.* **2024**, *14*, 3913–3921. [CrossRef]
33. Guerrieri, M.; Parla, G. Real-time social distance measurement and face mask detection in public transportation systems during the COVID-19 pandemic and post-pandemic Era: Theoretical approach and case study in Italy. *Transp. Res. Interdiscip. Perspect.* **2022**, *16*, 100693. [CrossRef]
34. Shrimali, S.; Teuscher, C. A Novel Deep Learning-, Camera-, and Sensor-Based System for Enforcing Hand Hygiene Compliance in Healthcare Facilities. *IEEE Sens. J.* **2023**, *23*, 13659–13670. [CrossRef]
35. Buachoom, A.; Thedsakhulwong, A.; Wuttiprom, S. An Arduino board with ultrasonic sensor investigation of simple harmonic motion. *J. Phys. Conf. Ser.* **2019**, *1380*, 012098. [CrossRef]
36. Ashjaei, M.; Khalilzad, N.; Mubeen, S.; Behnam, M.; Sander, I.; Almeida, L.; Nolte, T. Designing end-to-end resource reservations in predictable distributed embedded systems. *Real-Time Syst.* **2017**, *53*, 916–956. [CrossRef]
37. Sciangula, G.; Casini, D.; Biondi, A.; Scordino, C.; Di Natale, M. End-To-end response-time analysis of DDS-based real-time applications. *Internet Things* **2026**, *36*, 101853. [CrossRef]
38. Holtmann, J.; Deantoni, J.; Fockel, M. Early timing analysis based on scenario requirements and platform models. *Softw. Syst. Model.* **2022**, *21*, 2171–2211. [CrossRef]
39. Kim, J.-I.; Gang, H.-S.; Pyun, J.-Y.; Kwon, G.-R. Implementation of QR Code Recognition Technology Using Smartphone Camera for Indoor Positioning. *Energies* **2021**, *14*, 2759. [CrossRef]

40. Karrach, L.; Pivarčiová, E.; Božek, P. Identification of QR Code Perspective Distortion Based on Edge Directions and Edge Projections Analysis. *J. Imaging* **2020**, *6*, 67. [CrossRef] [PubMed]
41. Ahmed, W.; Hasan, O.; Tahar, S. Formalization of Reliability Block Diagrams in Higher-order Logic. *J. Appl. Log.* **2016**, *18*, 19–41. [CrossRef]
42. Moustafa, K.; Hu, Z.; Mourelatos, Z.P.; Baseski, I.; Majcher, M. System reliability analysis using component-level and system-level accelerated life testing. *Reliab. Eng. Syst. Saf.* **2021**, *214*, 107755. [CrossRef]

Disclaimer/Publisher's Note: The statements, opinions and data contained in all publications are solely those of the individual author(s) and contributor(s) and not of MDPI and/or the editor(s). MDPI and/or the editor(s) disclaim responsibility for any injury to people or property resulting from any ideas, methods, instructions or products referred to in the content.